Journal of The Electrochemical Society, **165** (9) D344-D353 (2018)
0013-4651/2018/165(9)/D344/10/$37.00 © The Electrochemical Society

Speciation Model of the Mo(VI)-Ni(II)-Citrate-S(VI)-N(III) Aqueous System for the Study of the Electrodeposition of Molybdenum and Nickel Oxides Films

J. Morales-Santelices, M. Colet-Lagrille, [z] and M. García-García

Department of Chemical Engineering, Biotechnology and Materials, Faculty of Physical and Mathematical Sciences, Universidad de Chile, Santiago, Región Metropolitana, Chile

A speciation model is proposed for the determination of the concentration of different species formed in an aqueous solution containing Mo(VI), Ni(II), citrate, ammonia and sulfate at 298 K, 10^5 Pa and variable pH and Mo(VI)/Ni(II) activity ratios. This solution is to be used as electrolyte in the electrodeposition process of thin films of Mo and Ni oxides, which appear to be a promising material for the fabrication of photo-anodes for water splitting in photo-electrochemical cells. The speciation model comprises 53 species and their stability constants, which are related through molar and charge balances to estimate the composition of the solution given a pH value and formal concentrations. As a result, predominance and distribution diagrams are produced, based on which electrolyte conditions (pH and central species concentrations) are recommended to maximize the availability of desired species for the electrodeposition process. Eh-pH diagrams for molybdenum and nickel species at the recommended activities (10^{-2} for Mo and Ni species, and 10^{-1} for citrate, ammonia and sulfate species) are also produced, to determine the adequate potential range to be applied for the electrodeposition of Mo and Ni oxides films.
 [DOI: 10.1149/2.0191809jes]

Manuscript submitted March 9, 2018; revised manuscript received May 4, 2018. Published June 1, 2018.

Molybdenum oxides have recently emerged as a promising alternative in the search of new semiconductor materials to fabricate photo-electrodes for driving the water splitting reaction (WSR).[1,2] It has been reported that some compounds of the MoO_x family present: (i) n-type semiconduction;[3] (ii) relative band edge positions in aqueous electrolytes[4] and bandgap energy values[3,5] ($E_g > 1.23$ eV) suitable for harvesting enough energy to drive the oxygen evolution reaction (OER) in a water splitting photo-electrochemical cell.[4–6] In addition, molybdenum presents three stable oxidation states (+4 to +6), which is a desirable property for a catalytic surface in electron transfer mediated processes.[7]

Electrodeposition provides a simple, cheap, scalable and manufacturable fabrication method of semiconducting materials.[8] In this context, it is widely accepted that factors such as the electrolyte properties (concentrations of precursors and other compounds dissolved, solvent, pH), the type of substrate, and the electrodeposition parameters (electrode potential, current density, time), influence the morphological and photo-electrochemical properties of the generated semiconducting deposits (films).[8,9] The understanding of the thermodynamic stability of the aqueous electrolyte involved is crucial for the engineering of these parameters, and thus reaching higher solar-to-hydrogen conversion efficiencies (STH) in photo-electrochemical cells containing these photo-electrodes.[10]

In parallel with the studies on the photo-electrochemical applications of molybdenum oxides, the use of nickel as a catalyst has stood out during the last years, with several applications.[11] It is known that the presence of nickel in electrodes provides catalytic activity for both the OER and the hydrogen evolution reaction (HER) in aqueous solution,[12] which in addition with the properties stated above for molybdenum oxides makes attractive the idea of studying photo-electrodes based on mixed molybdenum-nickel oxides.

The co-deposition of nickel(II) with molybdenum(VI) in aqueous media at cathodic potentials has been previously reported.[13,14] Citrate has been added to aqueous electrolytes used in both nickel and molybdenum electrodeposition in several works,[15–18] because of its complexing ability[19,20] which allows to increase the solubility of metals. Besides, citrate is a weak polyprotic acid and therefore acts as a buffer.[21] It has also been stated that citrate interferes favorably in the mechanism of the co-deposition of nickel and molybdenum.[15] Similarly to the addition of citrate, ammonia is added to these electrolytes following the same logic: the formation of nickel complexes[22] and an increase of the solution buffering capacity in more alkaline conditions with respect to what citrate can do by itself.

The objective of this work is to develop a speciation model with thermodynamic data of the Mo(VI), Ni(II), citrate, sulfate and ammonia aqueous system. This model aims to determine the equilibrium concentrations of different species in solution to produce predominance and distribution diagrams. In addition, Eh-pH diagrams are produced for molybdenum and nickel species based on the speciation model results. All these diagrams are useful for choosing the most favorable electrolyte composition and the potential to be applied for the electrodeposition of molybdenum and nickel oxides films.

It should be noted that the thermodynamic results presented in this work are also useful for the study of the electrodeposition of molybdenum-nickel metal alloys, which are of interest in areas as diverse as corrosion protection and catalysis.[13–16]

Model Description

Speciation model.—The speciation model consists of a set of molar and charge balances, which comprises a system of non-linear equations whose inputs are the pH and the moles of each compound added to the electrolyte per kilogram of pure water. Using a set of equilibrium constants at 298 K, 10^5 Pa and in the limit of zero ionic strength[a], a computational routine was developed to solve this system of equations and determine the composition of the electrolyte at the thermodynamic equilibrium as schematized in Figure 1.

The 53 species included in the speciation model are enumerated in Table I and classified in Figure 2[b]. Each of them is associated with: a number, a reversible reaction in aqueous medium and an equilibrium constant. The stoichiometric coefficients and pK values[23–27] are associated with a generic hydrolysis reaction which involves a species

[a]The constants that were reported in media with ionic strength different from zero were extrapolated using the following equation presented in the OCDE Guidelines for the Extrapolation to Zero Ionic Strength:[29]

$$pK_J(I_m = 0) = pK_J(I_m) - \left(A\frac{\sqrt{I_m}}{1+\sqrt{I_m}} - 0.3\sqrt{I_m}\right)\sum_j \upsilon_j z_j^2$$

where υ_j are the stoichiometric coefficients associated to the reaction linked to species J, and z_j the unitary charge of each of the aqueous species involved in this equilibrium. pK values obtained this way are marked with an asterisk in Table I.

[b]The notation for molybdenum-citrate complexes is taken from the work of Cruywagen, Rohwer and Wessels.[24] [p,q,r] stands for the product of the reaction: p $MoO_{4(aq)}^{2-}$ + q $Hcit_{(aq)}^{3-}$ + r $H_{(aq)}^{+}$ ↔ $[p, q, r]_{(aq)}^{[2p+3q-r]-}$

[z]E-mail: mcolet@ing.uchile.cl

Table I. Species considered in the speciation model, their pK and stoichiometric matrix.

				R								
J	species	phase	z_j	ν_1	ν_2	ν_3	ν_4	ν_5	ν_6	ν_7	pK_J	references
1	H_2O	l	0	1	0	0	0	0	0	0	0	-
2	$Hcit^{3-}$	aq	−3	0	1	0	0	0	0	0	0	-
3	MoO_4^{2-}	aq	−2	0	0	1	0	0	0	0	0	-
4	Ni^{2+}	aq	+2	0	0	0	1	0	0	0	0	-
5	NH_3	aq	0	0	0	0	0	1	0	0	0	-
6	SO_4^{2-}	aq	−2	0	0	0	0	0	1	0	0	-
7	H^+	aq	+1	0	0	0	0	0	0	1	0	-
8	OH^-	aq	−1	1	0	0	0	0	0	−1	−14.0	24
9	$Ni_4(OH)_4^{4+}$	aq	+4	4	0	0	4	0	0	−4	−27.52	26
10	$NiOH^+$	aq	+1	1	0	0	1	0	0	−1	−9.54	26
11	$Ni(OH)_3^-$	aq	−1	3	0	0	1	0	0	−3	−29.2	26
12	Ni_2OH^{3+}	aq	+3	1	0	0	2	0	0	−1	−10.6	26
13	$[1, 1, 1]^{4-}$	aq	−4	0	1	1	0	0	0	1	8.55	25*
14	$[1, 1, 2]^{3-}$	aq	−3	0	1	1	0	0	0	2	14.39	25*
15	$[1, 1, 3]^{2-}$	aq	−2	0	1	1	0	0	0	3	18.40	25*
16	$[1, 1, 4]^-$	aq	−1	0	1	1	0	0	0	4	19.49	25*
17	$[1, 2, 4]^{4-}$	aq	−4	0	2	1	0	0	0	4	24.32	25*
18	$[1, 2, 5]^{3-}$	aq	−3	0	2	1	0	0	0	5	27.71	25*
19	$[1, 2, 6]^{2-}$	aq	−2	0	2	1	0	0	0	6	30.90	25*
20	$[2, 1, 3]^{4-}$	aq	−4	0	1	2	0	0	0	3	21.32	25*
21	$[2, 1, 4]^{3-}$	aq	−3	0	1	2	0	0	0	4	25.68	25*
22	$[2, 1, 5]^{2-}$	aq	−2	0	1	2	0	0	0	5	29.70	25*
23	$[2, 2, 4]^{6-}$	aq	−6	0	2	2	0	0	0	4	31.63	25*
24	$[2, 2, 5]^{5-}$	aq	−5	0	2	2	0	0	0	5	35.25	25*
25	$[2, 2, 6]^{4-}$	aq	−4	0	2	2	0	0	0	6	38.45	25*
26	$[4, 2, 9]^{5-}$	aq	−5	0	2	4	0	0	0	9	58.93	25*
27	$[4, 2, 10]^{4-}$	aq	−4	0	2	4	0	0	0	10	61.84	25*
28	$[4, 4, 11]^{9-}$	aq	−9	0	4	4	0	0	0	11	79.28	25*
29	$Ni(NH_3)^{2+}$	aq	+2	0	0	0	1	1	0	0	2.72	27
30	$Ni(NH_3)_2^{2+}$	aq	+2	0	0	0	1	2	0	0	4.89	27
31	$Ni(NH_3)_3^{2+}$	aq	+2	0	0	0	1	3	0	0	6.55	27
32	$Ni(NH_3)_4^{2+}$	aq	+2	0	0	0	1	4	0	0	7.67	27
33	$Ni(NH_3)_5^{2+}$	aq	+2	0	0	0	1	5	0	0	8.34	27
34	$Ni(NH_3)_6^{2+}$	aq	+2	0	0	0	1	6	0	0	8.31	27
35	$NiHcit^-$	aq	−1	0	1	0	1	0	0	0	6.76	24
36	NiH_2cit	aq	0	0	1	0	1	0	0	1	10.52	24
37	NiH_3cit^+	aq	+1	0	1	0	1	0	0	2	13.19	24
38	$Ni_2(OH)_2H_2cit_2^{4-}$	aq	−4	2	2	0	2	0	0	−2	3.85	24
39	NH_4^+	aq	+1	0	0	0	0	1	0	1	9.24	27
40	H_4cit	aq	0	0	1	0	0	0	0	3	14.27	28
41	H_3cit^-	aq	−1	0	1	0	0	0	0	2	11.14	28
42	H_2cit^{2-}	aq	−2	0	1	0	0	0	0	1	6.36	28
43	$Mo_7O_{24}^{6-}$	aq	−6	−4	0	7	0	0	0	8	52.81	24
44	$HMo_7O_{24}^{5-}$	aq	−5	−4	0	7	0	0	0	9	59.0	24
45	$H_2Mo_7O_{24}^{4-}$	aq	−4	−4	0	7	0	0	0	10	63.98	24
46	$H_3Mo_7O_{24}^{3-}$	aq	−3	−4	0	7	0	0	0	11	67.43	24
47	H_2MoO_4	aq	0	0	0	1	0	0	0	2	8.39	24
48	$HMoO_4^-$	aq	−1	0	0	1	0	0	0	1	4.09	24
49	HSO_4^-	aq	−1	0	0	0	0	0	1	1	1.99	27
50	$NiSO_4$	aq	0	0	0	0	1	0	1	0	2.35	26
51	Na^+	aq	+1	0	0	0	0	0	0	0	-	-
52	MoO_3	s	0	−1	0	1	0	0	0	2	11.68	24
53	β-$Ni(OH)_2$	s	0	2	0	0	1	0	0	−2	−11.03	24

*Extrapolated from non-zero ionic strength (see footnote a)

J and 7 central species: 5 master species ($Hcit^{3-}_{(aq)}$, $MoO^{2-}_{4(aq)}$, $Ni^{2+}_{(aq)}$, $NH_{3(aq)}$, $SO^{2-}_{4(aq)}$) plus $H^+_{(aq)}$ and $H_2O_{(l)}$:

$$J_{(aq)} \leftrightarrow \nu_1 H_2O_{(l)} + \nu_2 Hcit^{3-}_{(aq)} + \nu_3 MoO^{2-}_{4(aq)} + \nu_4 Ni^{2+}_{(aq)} + \nu_5 NH_{3(aq)} + \nu_6 SO^{2-}_{4(aq)} + \nu_7 H^+_{(aq)} \quad [1]$$

The following assumptions were made:

1. The system is closed: the total concentrations of Mo(VI), Ni(II), N(III), S(VI) and citrate are held invariable.
2. Vaporization of any compound is negligible.
3. No redox reactions take place in the aqueous solution.
4. The pH is adjusted by means of the addition of NaOH.

The expressions for the law of mass action of the reactions linked to aqueous non-spectator species (2 to 50) can be expressed in matrix

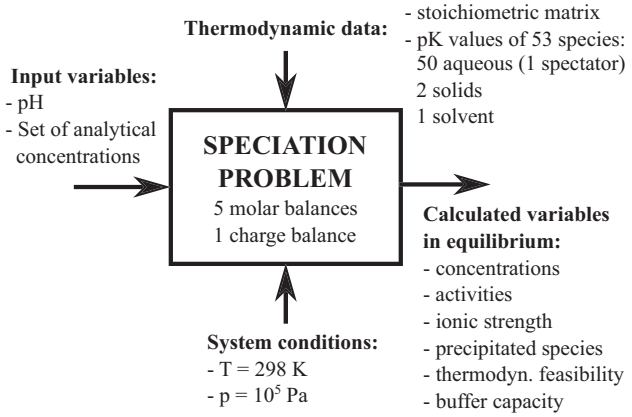

Figure 1. Input/output diagram for the speciation model developed.

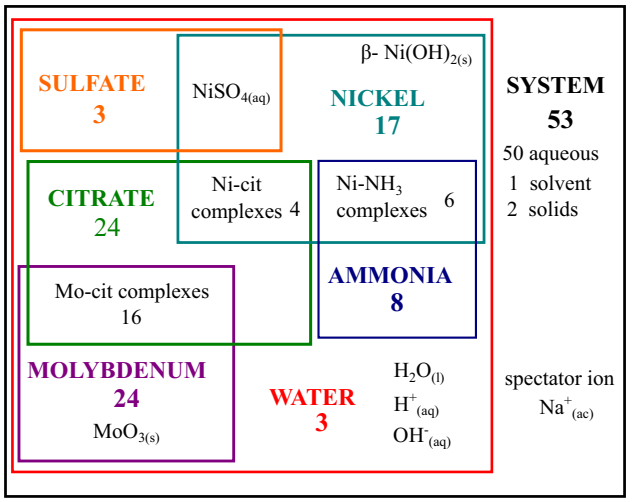

Figure 2. Description of the aqueous system studied. The species listed in Table I are here classified.

notation as follows (see List of Symbols):

$$pK_{2-50} = R_{2-50c}pa_{1-7} - pa_{2-50} \quad [2]$$

The activities of the aqueous species can be written in function of their molalities and activity coefficients:

$$pa_{2-51} = p\gamma_{2-51} + pb_{2-51} \quad [3]$$

where $p\gamma_J$ can be modelled by the Davies equation:[28]

$$p\gamma_{2-51} = A\left(\frac{\sqrt{I_m}}{1+\sqrt{I_m}} - 0.3I_m\right)[z_{2-51}, z_{2-51}] \quad [4]$$

A is the Debye-Hückel constant at the specific solvent and temperature (for water at 298 K and 10^5 Pa, A = 0.509 $mol^{0.5}$ $kg^{-0.5}$),[29] z_J is the unitary charge of the species J and I_m is the ionic force of the solution in molality scale, defined as:

$$I_m = \frac{1}{2}\langle[z_{2-51}, z_{2-51}], b_{2-51}\rangle \quad [5]$$

The 5 molar balances solved are these of citrate, molybdenum(VI), nickel(II), nitrogen(III) and sulfur(VI). These molar balances (equations) comprises terms for aqueous species but also for solid species that could appear because of precipitation (two solid species according to Table I). Each term in the mass balances represents the molality of a species in thermodynamic equilibrium and is expressed as a function of the molalities of the 5 central species, pK and pH values.

The charge balance assures that the electroneutrality condition is accomplished:

$$\langle z_{2-51}, b_{2-51}\rangle = 0 \quad [6]$$

Na^+ is the only spectator ion, as it does not participate in any expression of the law of mass action. However, its molality can be obtained throughout Equation 6.

In this model, the solvent activity is approximated to unity.

The molar balances depend on whether any (or both) of the solid species precipitate or not. This condition is determined as follows. Initially, a first balance is solved under the hypothesis that no solid species are formed in the solution:

$$C_m = R^T_{2-50m}b_{2-50} \quad [7]$$

With these 5 equations plus the charge balance in Equation 6 the system is fully determined, and a solution value for each variable can be obtained. The action mass laws of heterogeneous equilibria are used to determine whether the solution reaches the saturation limit for either of the solid species:

$$pQ_{52-53} = R_{52-53c}pa_{1-7} \quad [8]$$

Using the activity values found with the first balance (solution of Equation 7 replaced in Equation 8), the heterogeneous reaction quotients $Q_{52\text{-}53}$ can be obtained, and can be compared with $K_{52\text{-}53}$. Four cases are possible, and each one leads to a different S switch vector value:

i. if $Q_{52} \leq K_{52}$ and $Q_{53} \leq K_{53} \Rightarrow$ No solids are formed, $S = (0\ 0)^T$
ii. if $Q_{52} > K_{52}$ and $Q_{53} \leq K_{53} \Rightarrow$ Mo oxide precipitates, $S = (1\ 0)^T$
iii. if $Q_{52} \leq K_{52}$ and $Q_{53} > K_{53} \Rightarrow$ Ni hydroxide precipitates, $S = (0\ 1)^T$
iv. if $Q_{52} > K_{52}$ and $Q_{53} > K_{53} \Rightarrow$ Both species precipitate, $S = (1\ 1)^T$

Once the hypothesis is tested, a second molar balance is solved, now including the solid species. For the latter, $b_{52,53}$ stands for the moles of the precipitated species per kilogram of water:

$$C_m = R^T_{2-50m}b_{2-50} + R^T_{52-53m}[S, b_{52-53}] \quad [9]$$

Note that for case (i), the unsaturated solution, Equation 9 corresponds to Equation 7. When a species precipitates, the activity of the associated metal aqueous master species is fixed, and it comes from its respective heterogeneous equilibrium expression. This means that in the case that molybdenum precipitates, pa_3 is obtained by the mass action law of reaction 52 and likewise does Ni with reaction 53. Despite of adding new restrictions to the problem, new variables have been added in each case (the amount of precipitated solids: b_{52} and/or b_{53}), so the problem keeps being fully determined and a solution can be obtained. The degree of freedom analysis used for the resolution of the system of equations is summarized in Table II.

Table II. Degree of freedom analysis.

case	independent equations	fixed parameters	independent variables
I	5 mass balances + 1 charge balance	pH, $pK_{1\text{-}53}$, C_m	$b_{2\text{-}6}$, b_{51}
II			b_2, $b_{4\text{-}6}$, $b_{51\text{-}52}$
III			$b_{2,3}$, $b_{5,6}$, b_{51}, b_{53}
IV			b_2, $b_{5,6}$, $b_{51\text{-}53}$

Table III. Thermodynamic data of species considered in the Eh-pH diagrams of molybdenum and nickel.

species	phase	$\Delta_f G^o$ / kJ mol^{-1}	references	species	phase	$\Delta_f G^o$ / kJ mol^{-1}	references
H_2O	l	−237.140	25	$Ni(NH_3)^{2+}$	aq	−56.920	26‡
$Hcit^{3-}$	aq	−1 162.258	30	$Ni(NH_3)_2^{2+}$	aq	−71.207	26‡
MoO_4^{2-}	aq	−838.500	31	$Ni(NH_3)_3^{2+}$	aq	−88.404	26‡
Ni^{2+}	aq	−45.773	25	$Ni(NH_3)_4^{2+}$	aq	−108.685	26‡
NH_3	aq	−26.673	25	$Ni(NH_3)_5^{2+}$	aq	−131.533	26‡
SO_4^{2-}	aq	−744.004	25	$Ni(NH_3)_6^{2+}$	aq	−158.377	26‡
H^+	aq	0	25	$NiHcit^-$	aq	−1 246.617	25
$Ni_4(OH)_4^{4+}$	aq	−974.567	25	NiH_2cit	aq	−1 268.079	25
$NiOH^+$	aq	−228.458	25	NiH_3cit^+	aq	−1 283.320	25
$Ni(OH)_3^-$	aq	−590.519	25	$Ni_2(OH)_2H_2cit_2^{4-}$	aq	−2 912.318	23‡
Ni_2OH^{3+}	aq	−268.181	25	$Mo_7O_{24}^{6-}$	aq	−4 633.538	32‡
$[1, 1, 1]^{4-}$	aq	−2 049.582	24‡§	$HMo_7O_{24}^{5-}$	aq	−4 594.387	32‡
$[1, 1, 2]^{3-}$	aq	−2 082.892	24‡§	$H_2Mo_7O_{24}^{4-}$	aq	−4 562.992	32‡
$[1, 1, 3]^{2-}$	aq	−2 105.776	24‡§	$H_3Mo_7O_{24}^{3-}$	aq	−4 541.474	32‡
$[1, 1, 4]^-$	aq	−2 112.014	24‡§	H_2MoO_4	aq	−790.610	23
$[1, 2, 4]^{4-}$	aq	−3 301.846	24‡§	$HMoO_4^-$	aq	−815.040	32‡
$[1, 2, 5]^{3-}$	aq	−3 321.171	24‡§	$NiSO_4$	aq	−803.191	25
$[1, 2, 6]^{2-}$	aq	−3 339.375	24‡§	MoO_3	s	−669.742	32‡
$[2, 1, 3]^{4-}$	aq	−2 960.969	24‡§	β-$Ni(OH)_2$	s	−457.100	25
$[2, 1, 4]^{3-}$	aq	−2 985.831	24‡§	O_2	g	0	25
$[2, 1, 5]^{2-}$	aq	−3 008.772	24‡§	MoO_2	s	−533.010	23
$[2, 2, 4]^{6-}$	aq	−4 182.065	24‡§	Ni	s	0	25
$[2, 2, 5]^{5-}$	aq	−4 198.153	24‡§	$Ni(OH)_3$	s	−541.800	31
$[2, 2, 6]^{4-}$	aq	−4 220.996	24‡§	Ni_2H	s	11.800	33
$[4, 2, 9]^{5-}$	aq	−6 031.497	24‡§	NiOOH	s	−409.258	34
$[4, 2, 10]^{4-}$	aq	−6 014.876	24‡§	—	-	—	-
$[4, 4, 11]^{9-}$	aq	−8 455.577	24‡§	—	-	—	-

‡Calculated from a reported pK value and the values of the standard molar Gibbs energy of formation shown in this table
§Extrapolated from a non-zero ionic strength (see footnote a)

Eh-pH diagrams model.—A selected set of species of different oxidation states and their standard molar Gibbs energy of formation were chosen from literature and are listed in Table III.[23–26,30–34] The method used to generate the Eh-pH diagrams for molybdenum and nickel species is described in detail elsewhere.[35] The results obtained were complemented with these produced with the speciation model for Mo(VI) and Ni(II) species.

Model Resolution

Speciation model.—The mathematical model described in the previous section was implemented and solved using MATLAB 2017, for the species concentrations listed in Table IV. The concentrations of citrate and ammonia are fixed arbitrarily in order to provide an adequate electrical conductivity to the solution (as shown in the Results and discussion section).

Eh-pH diagrams model.—The calculations for the construction of the Eh-pH diagrams of molybdenum and nickel species were performed in MATLAB 2017 using the thermodynamic data summarized in Table III, for the same temperature and total pressure set in the speciation model (298 K and 10^5 Pa). The activities of the non-central species listed in Table III, $MoO_{4(aq)}^{2-}$ and $Ni_{(aq)}^{2+}$ are set at 10^{-2}, and these of citrate, ammonia and sulfate species are equal to 10^{-1}. The solvent and solids activities are equal to unity. The pH span used is from 0 to 14, and the Eh span is set between −1.5 and +1.5 V vs SHE.

Results and Discussion

Predominance diagrams.—The system of equations described in the Speciation model section was solved using a grid of 56 × 141 points, varying the pH, $pC_{Mo(VI)}$ and $pC_{Ni(II)}$ values. The concentrations of the other master species (citrate, N(III) and S(VI)) were held constant and equal to 0.1 mol (kg H_2O)$^{-1}$, as shown in Table IV. The predominance diagrams produced (Figures 3a–3e) consider a Mo(VI)/Ni(II) concentration ratio equal to 1.0, in the concentration range shown in Table IV. Each zone is associated with the pH-pC pairs in which the labeled species presents the highest molality in thermodynamic equilibrium.

Figure 4 shows plots for the amount of alkali added (Figure 4a) and the ionic strength of the electrolyte (Figure 4b) within the span of pH and pCs used in the predominance diagrams. It is important to mention that, the electroneutrality condition cannot be fulfilled in the area marked in grey in Figure 4a without including an additional anionic species to the system. Therefore, in principle, the speciation model here presented could only be valid in the region outside this area.

The predominance diagram for Mo(VI) species (Figure 3a) can be divided in four main areas: (i) at very acidic conditions the metal precipitates as an oxide ($MoO_{3(s)}$); (ii) in mildly acidic conditions polyisomolybdates take importance when the amount of Mo(VI) exceeds the amount of citrate (at values of $pC_{Mo(VI)}$ below 1.0); (iii) when the relation is inverted ($pC_{Mo(VI)}$ above 1.0) the citrate-molybdate complexes predominate; and (iv) the molybdate ion ($MoO_{4(aq)}^{2-}$) is the most

Table IV. Values used for the speciation model resolution.

variable	value	units
total Mo, total Ni	variable, each from 10^{-3} to $10^{-0.25}$	mol (kg H_2O)$^{-1}$
pH	variable, from 0 to 14	-
total citrate	0.10	mol (kg H_2O)$^{-1}$
total N	0.10	mol (kg H_2O)$^{-1}$
total S	0.10	mol (kg H_2O)$^{-1}$

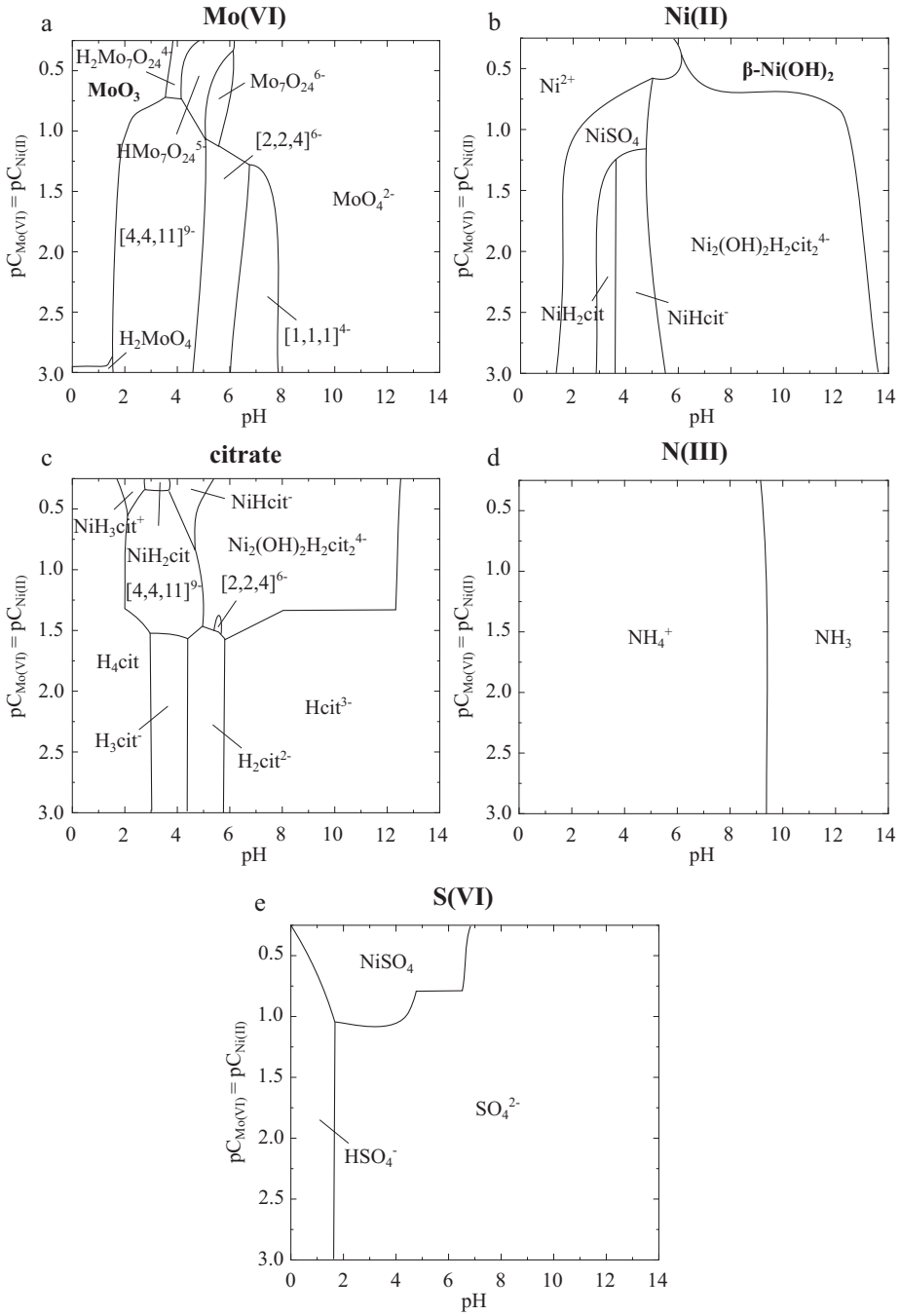

Figure 3. Predominance diagrams of: (a) molybdenum, (b) nickel, (c) citrate, (d) ammonia and (e) sulfur. $pC_{Mo(VI)}$ and $pC_{Ni(II)}$ have equal values and vary simultaneously. Solid species are showed in bold letter.

stable species under neutral and alkaline conditions. These results are consistent with previous studies of the Mo(VI)-H_2O system and show a big similarity in the predominance zone of polyisomolybdates.[36–39]

The predominance diagram for Ni(II) species (Figure 3b) is strongly marked by the formation of nickel-citrate complexes in different states of protonation ($NiH_2cit_{(aq)}$, $NiHcit^-_{(aq)}$) and the dimeric nickel-citrate form: $[Ni_2(OH)_2H_2cit_2]^{4-}_{(aq)}$. In acid and diluted conditions, Ni is present as aqueous nickel sulfate ($NiSO_{4(aq)}$). When the activity of the protons is too high (pH < 3.0) citrate tends to be fully protonated (Figure 3c), forming citric acid ($H_4cit_{(aq)}$) and avoiding the coordinate bonds with nickel, thus making favorable the formation of free nickel ion ($Ni^{2+}_{(aq)}$). At more basic pH (ca. pH = 6.0), the stability of the dimeric nickel-citrate form is high, thus the formation of solid nickel hydroxide (β-$Ni(OH)_{2(s)}$) is negligible in comparison to results presented in the literature for the Ni-H_2O system.[40]

The predominance diagram for citrate (Figure 3c) shows that it forms complexes in a wide range of pH at pC values for molybdenum and nickel above 1.5. Ni-cit complexes show more stability than Mo-cit complexes, except for a small region in acidic conditions (pH < 5.0; 0.5 < pC < 1.5). The stability of the dimeric nickel-citrate form is such that it predominates in neutral and moderately alkaline media (5.0 < pH < 12). However, when the metals concentration is low, free citrate in its different states of protonation prevails.

The predominance diagram for N(III) species (Figure 3d) does not exhibit sensibility to the presence of molybdenum and nickel in solution. Despite of the capability of ammonia ($NH_{3(aq)}$) to form complexes with Ni(II) (see Table I), the free ionic form of nickel ($Ni^{2+}_{(aq)}$) prevails in very acidic media, since ammonia is protonated ($NH^+_{4(aq)}$) and thus unable to form a coordinate bond. In addition, the presence of a stronger ligand such as citrate makes the concentration of the nickel-

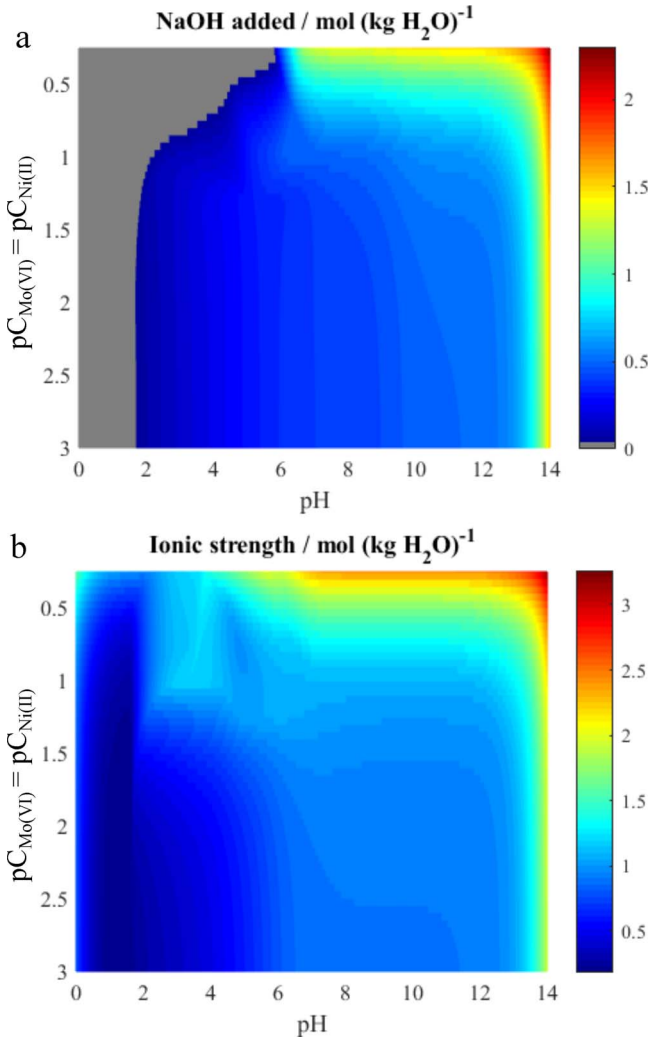

Figure 4. (a) Amount of NaOH added to the aqueous system. The grey area corresponds to the unfeasible zone at which a negative concentration of NaOH should be added. (b) Ionic strength of the electrolyte.

ammonia complexes negligible in the more basic region. Therefore, as this compound does not bind strongly to Ni(II) or Mo(VI), ammonia can be added to the system to regulate pH in the basic region without interfering considerably in the hydrolysis equilibria.

Finally, the predominance diagram for S(VI) species (Figure 3e) shows that the most stable form is sulfate ($SO^{2-}_{4(aq)}$), and in very acidic media (pH < 2.0) the stable form is bisulfate ($HSO^{-}_{4(aq)}$). Nevertheless, nickel sulfate ($NiSO_{4(aq)}$) predominates at acid pH values and high concentration of Ni ($pC_{Ni(II)} < 1.1$), which explains the formation of the Mo-cit complex $[4, 4, 11]^{9-}_{(aq)}$ observed around these conditions (Figure 3c).

The ionic strength (Figure 4b) of the system tends to increase with pH, because of the presence of highly charged anionic species (such as $MoO^{2-}_{4(aq)}$, $Hcit^{3-}_{(aq)}$ and $SO^{2-}_{4(aq)}$) and the increasing amount of NaOH added to the system, as can be seen in Figure 4a.

Electrolyte conditions for the electrodeposition of molybdenum-nickel oxide films.—The predominance diagrams obtained are useful to identify adequate species concentrations and pH of the electrolyte to be used for the electrodeposition of molybdenum and nickel oxides. Some recommendations produced from the previous analysis are listed below:

1. *Maximization of the free Mo(VI) activity available for electrodeposition*. As the main electrodeposition reactions of molybdenum oxide are thought to be:[41,42]

$$MoO^{2-}_{4(aq)} + 2H_2O_{(l)} + 2e^- \rightarrow MoO_{2(s)} + 4OH^-_{(aq)} \quad [10]$$

$$2MoO^{2-}_{4(aq)} + 3H_2O_{(l)} + 2e^- \rightarrow Mo_2O_{5(s)} + 6OH^-_{(aq)} \quad [11]$$

pH is preferred to be alkaline because of the higher amount of molybdate ion, $MoO^{2-}_{4(aq)}$, present in the solution. Unfortunately, a basic environment increases the availability of $OH^-_{(aq)}$ in the system and hence, due to the Le Châtelier's principle applied to Reactions 10 and 11, more cathodic potentials have to be applied to achieve the reduction of Mo(VI). A pH > 8.0 would assure that molybdate ion is the predominant molybdenum form at any pC value. Lower values of $pC_{Mo(VI)}$ would also imply a higher molality of $MoO^{2-}_{4(aq)}$.

2. *Precipitation of Mo(VI)*. $MoO_{3(s)}$ is formed in acidic media. The presence of citrate in a higher concentration than molybdenum provokes a decrease in the critical pH below which the oxide is formed. It is recommendable then to have $pC_{Mo(VI)}$ values higher than pC_{cit} values.
3. *Polyisomolybdates formation*. Since these species are big and highly-negative charged, they are not desirable for reduction processes. The use of alkaline pH avoids this problem.
4. *Precipitation of Ni(II)*. As β-$Ni(OH)_{2(s)}$ is formed in very alkaline media, values of pH above 12 should be avoided. In the same logic, analogically to molybdenum, it is recommendable to have $pC_{Ni(II)}$ values higher than pC_{cit} values to avoid Ni(II) precipitation.
5. *Mass transfer coefficients of electroactive species*. Both molybdenum and nickel species are needed to be reduced. As molybdate ions are negatively charged, a smaller migrational flux of this species to the cathode should be observed when compared to the migrational flux of the positively charged species $Ni^{2+}_{(aq)}$. Consequently, both nickel and molybdenum predominant species should be chosen to have the same or a similar net charge, so the current efficiency of the electrodeposition process will be distributed more evenly between them. Dimeric form of the nickel-citrate complex complies with this requirement, which is the main form of Ni(II) in the pH range between 5.0 and 12.
6. *Ionic strength*. As reported in the literature,[43] a solution with high ionic force will have a low resistivity and, therefore, promotes smaller ohmic losses during the electrodeposition process. Higher ionic strengths are achieved with higher pH and low $pC_{Mo(VI)}$ and $pC_{Ni(II)}$ values. The ionic strength (I_m) keeps almost steady in the range of pH between 7.0 and 12.

In view of points 1 to 6, and the conditions reported in the literature for the electrodeposition of molybdenum oxides,[5,41,42] a recommended electrolyte condition for the co-deposition of molybdenum-nickel oxides films is pH = 9.0 and $pC_{Mo(VI)} = pC_{Ni(II)} = 2.0$. Figures 5a–5c shows the distribution diagrams for Mo(VI), Ni(II) and citrate at these pC values, which reassures that the main species of molybdenum and nickel in solution at these conditions would be molybdate ($MoO^{2-}_{4(aq)}$) and the dimeric form of the nickel-citrate complex ($[Ni_2(OH)_2H_2cit_2]^{4-}_{(aq)}$). In addition, Figure 5d shows that the main contributors to the ionic strength are sodium ($Na^+_{(aq)}$), sulfate ($SO^{2-}_{4(aq)}$) and $Hcit^{3-}_{(aq)}$ ions, all of which are mainly spectator ions during the electrodeposition process, and thus would maintain the conductivity of the solution.

From the previous discussion, it is clear that citrate has a significant role as complexing agent to increase the solubility of Mo(VI) and Ni(II), and to promote the formation of nickel-citrate complexes with a mass transfer coefficient comparable to that of molybdate ($MoO^{2-}_{4(aq)}$). To visualize better these effects, the speciation model was solved using a negligible total concentration of citrate (pC_{cit} = 6.0) and maintaining all the other conditions as stated in Table IV.

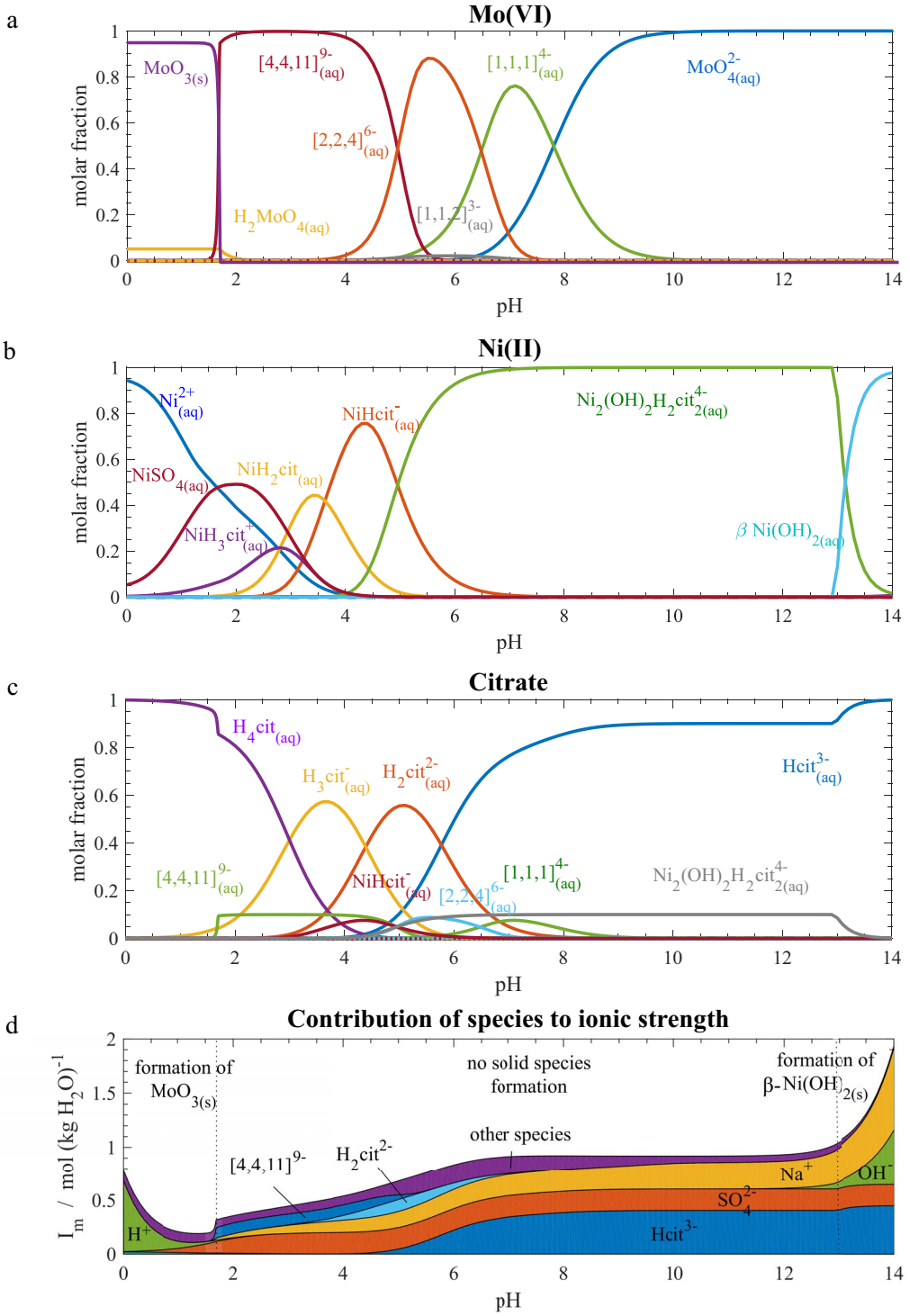

Figure 5. Distribution diagrams for the species of: (a) molybdenum, (b) nickel and (c) citrate, using $pC_{Mo(VI)} = pC_{Ni(II)} = 2.0$; (d) Contribution of species to the ionic strength of the solution.

Figures 6a–6c show the predominance diagrams obtained for Mo(VI), Ni(II) and citrate species, showing that in neutral-alkaline conditions (above $pC_{Mo(VI)} = pC_{Ni(II)} = 1.0$) the dimeric form of the nickel-citrate complex ($[Ni_2(OH)_2H_2cit_2]^{4-}_{(aq)}$) is replaced by $NiSO_{4(aq)}$ as the main Ni(II) species, and that β-$Ni(OH)_{2(s)}$ starts to precipitate for pH above 8.0. This is undesirable considering that above pH = 6.0, at which Mo(VI) is predominantly present as molybdate, the Ni(II) species present in solution would be mainly a neutral or a precipitated compound. This is confirmed by the distribution diagrams presented in Figures 6d–6e ($pC_{Mo(VI)} = pC_{Ni(II)} = 2.0$), in which molybdate is the main Mo(VI) species in solution at neutral and alkaline pH, and Ni(II) is present mainly as: (i) $NiSO_{4(aq)}$ and $Ni^{2+}_{(aq)}$ at pH between 6.0 and 8.0 and (ii) β-$Ni(OH)_{2(s)}$ at pH above 8.0. Furthermore, a lower concentration of citrate in the solution would also impact the conductivity of it, since $Hcit^{3-}_{(aq)}$ ions are main contributors to the ionic strength in alkaline conditions.

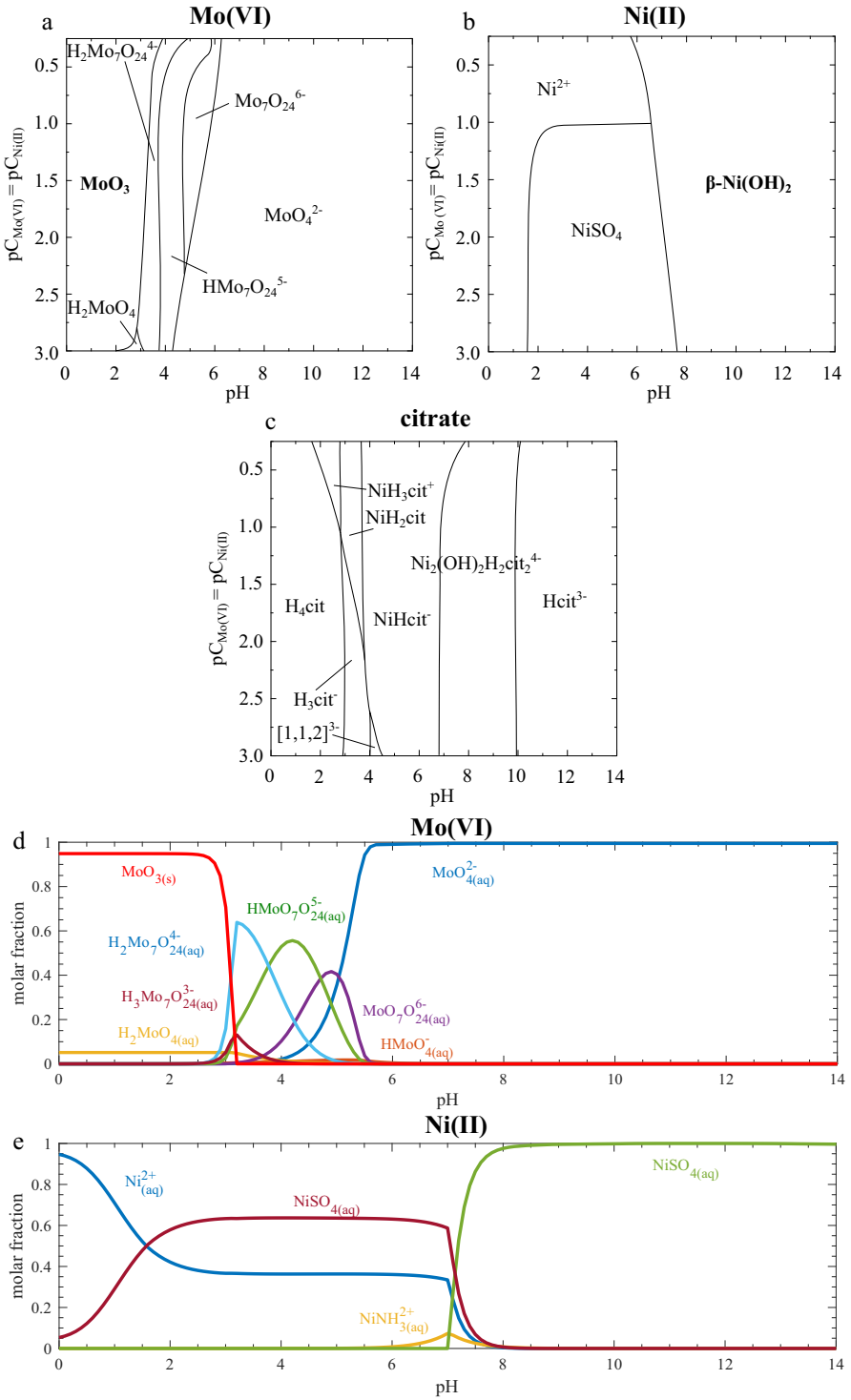

Figure 6. Predominance diagrams of: (a) molybdenum, (b) nickel and (c) citrate, using $pC_{cit} = 6.0$. Solid species are showed in bold letter. Distribution diagrams for the species of: (d) molybdenum and (e) nickel, using $pC_{cit} = 6.0$ and $pC_{Mo(VI)} = pC_{Ni(II)} = 2.0$. All the other concentrations correspond to those stated in Table IV.

Applied potential for the electrodeposition of molybdenum-nickel oxide films.—Eh-pH diagrams for nickel and molybdenum species (at 298 K and 10^5 Pa) were produced as stated in the Eh-pH Diagrams model section, for an activity equal to 10^{-2} for all nickel and molybdenum species and equal to 10^{-1} for citrate, ammonia and sulfate species. These diagrams are used here to determine the adequate potential to be applied for the electrodeposition of Mo-Ni oxides, though they can also be used for the study of the electrodeposition of Mo-Ni metal alloys.

Figure 7a shows the Eh-pH diagram obtained for molybdenum species, which confirms that at pH = 9.0 the main reduction reaction of molybdate ions ($MoO_{4(aq)}^{2-}$) is Reaction 10, to produce the desired molybdenum oxide ($MoO_{2(s)}$) product. In accordance with these results, the reduction of $MoO_{4(aq)}^{2-}$ to $MoO_{2(s)}$ would occur at an applied potential between −0.25 and −0.68 V vs SHE. However, Shembel et al. have reported that this electrodeposition reaction occurs solely at high overpotentials,[41] which indicates that a potential lower than −0.68 V vs SHE would need to be applied to promote the oxide formation.

The Eh-pH diagram obtained for nickel species (Figure 7b) shows that non-oxidized forms of nickel would be produced in this potential range. In fact, between −0.56 and −0.65 V vs SHE (at pH = 9.0) the

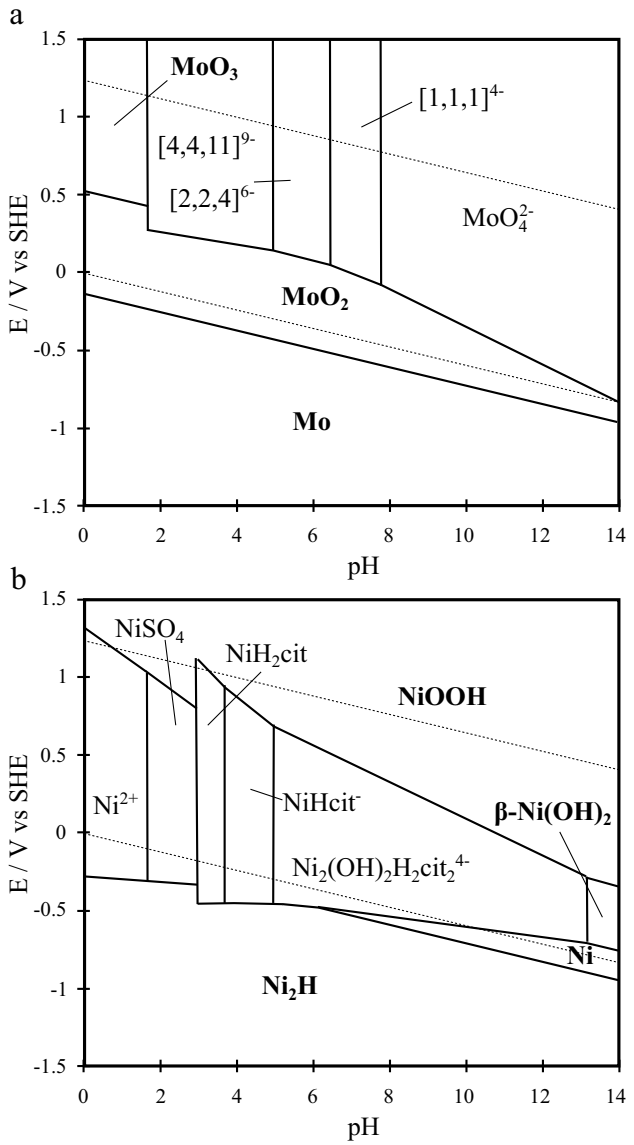

Figure 7. Eh-pH diagrams for (a) molybdenum and (b) nickel species at 298 K and 10^5 Pa. Activity of molybdenum and nickel species equal to 10^{-2} and activity of citrate, ammonia and sulfate species equal to 10^{-1}. Solid species are showed in bold letter.

most probable reduction reaction of the dimeric form of the nickel-citrate complex ($[Ni_2(OH)_2H_2cit_2]^{4-}_{(aq)}$) is:

$$\left[Ni_2(OH)_2H_2cit_2\right]^{4-}_{(aq)} + 4e^- \rightarrow 2Ni_{(s)} + 2OH^-_{(aq)} + 2Hcit^{3-}_{(aq)} \quad [12]$$

And below −0.65 V vs SHE, the nickel hydride ($Ni_2H_{(s)}$) would be preferentially formed:

$$\left[Ni_2(OH)_2H_2cit_2\right]^{4-}_{(aq)} + H_2O_{(l)} + 5e^- \rightarrow Ni_2H_{(s)} + 3OH^-_{(aq)} + 2Hcit^{3-}_{(aq)} \quad [13]$$

This indicates that applying a potential below −0.56 V vs SHE the co-electrodeposition of molybdenum oxide and nickel metal/nickel hydride would be promoted (in addition to the unavoidable hydrogen evolution at the cathode). However, to obtain a stable oxide film to be used as a photo-anode to drive the oxygen evolution reaction (OER) in a water splitting photo-electrochemical cell, a post-deposition calcination treatment should be assessed.

Conclusions

A speciation model for the Mo(VI)-Ni(II)-citrate-S(VI)-N(III)-H_2O system has been proposed and solved for a set of concentrations, varying the amount of Mo(VI) and Ni(II) and the pH of the solution, to obtain predominance and distribution diagrams. These plots were used to discuss and choose adequate conditions for the electrodeposition process of molybdenum and nickel oxides films, suggesting that a pH = 9.0 and $pC_{Mo(VI)} = pC_{Ni(II)} = 2.0$ are recommendable when $pC_{cit} = pC_{S(VI)} = pC_{N(III)} = 1.0$ is fixed. Additionally, Eh-pH diagrams for nickel and molybdenum species were obtained to determine the potential to be applied for the electrodeposition of molybdenum and nickel oxides. The results suggest that a potential below −0.56 V vs SHE must be applied to the cathode to obtain a MoO_2-Ni/Ni_2H deposit, which would need further post-calcination treatment to obtain a stable photo-anode for water splitting applications.

The thermodynamic modelling here presented and discussed is central for the characterization of the molybdenum-nickel oxides-based photo-anodes to be produced, as well as to establish the operating conditions under which these deposits would be stable. The analysis of the experimental results obtained in the light of this thermodynamic model is to be presented in a subsequent manuscript.

List of Symbols

Variables

Variable	Dimensions	Description	Units
a_{x-y}	$(y-x+1)\times 1$	activities in equilibrium from species x to y	-
b_{x-y}	$(y-x+1)\times 1$	aqueous molality in equilibrium from species x to y	mol kg H_2O^{-1}
C_m	5×1	formal concentration from master species (2 to 6)	mol kg H_2O^{-1}
I_m	1×1	electrolyte ionic force	mol kg H_2O^{-1}
J	1×1	index of a generic species	-
K_{x-y}	$(y-x+1)\times 1$	equilibrium constants from reactions associated to species x to y	-
pH	1×1	$-\log_{10}$ of proton activity	-
Q_{x-y}	$(y-x+1)\times 1$	reaction quotients associated to species x to y	-
R_{x-yc}	$(y-x+1)\times 7$	central species rows (ν_1 to ν_7) of the stoichiometric matrix associated to species x to y	-
R_{x-ym}	$(y-x+1)\times 5$	master species rows (ν_2 to ν_6) of the stoichiometric matrix associated to species x to y	-
S	2×1	switch vector for solubility products	-
z_{x-y}	$(y-x+1)\times 1$	unitary charge of aqueous species from species x to y	-

Greek variables

Variable	Size	Description	Units
γ_{x-y}	$(y-x+1)\times 1$	activity cofficients from species x to y	-
$\Delta_f G^o$	1×1	standard molar Gibbs energy of formation	kJ mol^{-1}
ν_x	1×1	stoichiometric coefficient associated to species x in hydrolysis reaction	-

Notation

Symbol	Meaning
⟨a, b⟩	dot product between a and b vectors
[a, b]	element by element product between a and b vectors
$_p$	$-\log_{10}$ taken element by element
$_T$	transposed vector or matrix

ORCID

M. Colet-Lagrille https://orcid.org/0000-0001-9630-3329

References

1. Y. Zhao, Y. Zhang, Z. Yang, Y. Yan, and K. Sun, *Sci. Technol. Adv. Mater.*, **14**, 043501 (2013).
2. D. O. Scanlon et al., *J. Phys. Chem. C*, **114**, 4636 (2010).
3. N. Dukstiene, D. Sinkeviciute, and A. Guobiene, *Cent. Eur. J. Chem.*, **10**, 1106 (2012).
4. N. Dukštiene and D. Sinkevičiute, *J. Solid State Electrochem.*, **17**, 1175 (2013).
5. R. S. Patil, M. D. Uplane, and P. S. Patil, *Appl. Surf. Sci.*, **252**, 8050 (2006).
6. R. van de Krol and M. Grätzel, *Photoelectrochemical Hydrogen Production*, Springer US, (2012) https://www.springer.com/gp/book/9781461413790.
7. D. Shriver, M. Weller, T. Overton, F. Armstrong, and J. Rourke, *Inorganic Chemistry*, 6th Ed., W.H. Freeman and Company, New York, (2014).
8. I. M. Dharmadasa and J. Haigh, *J. Electrochem. Soc.*, **153**, G47 (2006).
9. T. Li et al., *RSC Adv.*, **6**, 13914 (2016).
10. Z. Chen, H. Dinh, and E. Miller, *Photoelectrochemical Water Splitting: Standards, Experimental Methods, and Protocols*, Springer-Verlag New York, (2013) https://www.springer.com/gp/book/9781461482970.
11. V. P. Ananikov, *ACS Catal.*, **5**, 1964 (2015).
12. J. W. Schüttauf et al., *J. Electrochem. Soc.*, **163**, F1177 (2016).
13. C. Fan, D. L. Piron, S. Abderrahman, and P. Paradis, *J. Electrochem. Soc.*, **141**, 382 (1994).
14. E. J. Podlaha and D. Landolt, *J. Electrochem. Soc.*, **144**, 1672 (1997).
15. Z. Yue et al., *Chinese J. Chem.*, **18**, 29 (2000).
16. E. Chassaing, K. Vu Quang, and R. Wiart, *J. Appl. Electrochem.*, **19**, 839 (1989).
17. C. Li, X. Li, Z. Wang, and H. Guo, *Trans. Nonferrous Met. Soc. China*, **17**, 1300 (2007).
18. C. Li, X. Li, Z. Wang, and H. Guo, *Rare Met. Mater. Eng.*, **44**, 1561 (2015).
19. S. Ishibashi, H. Yokoyama, and K. Makioka, *Nippon kagaku zassi*, **82**, 442 (1961).
20. E. R. Still and P. Wikberg, *Inorganica Chim. Acta*, **46**, 147 (1980).
21. A. Apelblat, *Citric Acid*, Springer, (2015) https://www.springer.com/la/book/9783319112329.
22. E. F. Caldin, M. W. Grant, and B. B. Hasinoff, *J. Chem. Soc. Faraday Trans. 1 Phys. Chem. Condens. Phases*, **68**, 2247 (1972).
23. Amec Foster Wheeler, (2007) http://www.hatches-database.com/release.htm.
24. J. J. Cruywagen, E. A. Rohwer, and G. F. S. Wessels, *Polyhedron*, **14**, 3481 (1995).
25. H. Gamsjäger, J. Bugajski, T. Gajda, R. J. Lemire, and W. Preis, *Chemical Thermodynamics of Nickel*, OECD NEA Data Bank, (2005) https://www.oecd-nea.org/dbtdb/pubs/vol6-nickel.pdf.
26. A. Martell, *Critical Stability Constants Volume 4: Inorganic Complexes*, (1976) https://www.springer.com/gp/book/9781475755084.
27. R. Guillaumont et al., *Update on the Chemical Thermodynamics of Uranium, Neptunium, Plutonium, Americium and Technetium*, OECD NEA Data Bank, (2003) https://www.oecd-nea.org/dbtdb/pubs/vol5-update-combo.pdf.
28. C. W. Davies, *Ion Association*, Butterworth, Washington D.C., (1962).
29. I. Grenthe, F. Mompean, K. Spahiu, and H. Wanner, *Guidelines for the Extrapolation To Zero Ionic Strength*, (2013) https://www.oecd-nea.org/dbtdb/guidelines/tdb2.pdf.
30. W. Hummel, G. Anderegg, L. Rao, I. Puigdomenech, and O. Tochiyama, *Chemical Thermodynamics of Compounds and Complexes of U, Np, Pu, Am, Tc, Se, Ni and Zr with Selected Organic Ligands*, OECD NEA Data Bank, (2005) https://www.oecd-nea.org/dbtdb/pubs/vol9-organic-ligands.pdf.
31. A. J. Bard, R. Parsons, and J. Jordan, *Standard Potentials in Aqueous Solution*, International Union of Pure and Applied Chemistry (IUPAC), New York, U.S.A., (1985).
32. U.S. Geological Survey (USGS), (2015) https://wwwbrr.cr.usgs.gov/projects/GWC_coupled/phreeqc/.
33. B. Beverskog and I. Puigdomenech, *Corros. Sci.*, **39**, 969 (1997).
34. C. W. Bale and E. Bélisle, (2014) http://www.crct.polymtl.ca/compweb.php.
35. E. D. J. Verink, in *Uhlig's Corrosion Handbook*, p. 93, Wiley, New Jersey, U.S.A. (2011).
36. K. H. Gayer, *J. Chem. Educ.*, **54**, A429 (1977).
37. T. Ozeki, H. Kihara, and S. Hikime, *Anal. Chem.*, **59**, 945 (1987).
38. T. Ozeki, H. Kihara, and S. Ikeda, *Anal. Chem.*, **60**, 2055 (1988).
39. P. C. H. Mitchell, *Speciation of Molybdenum Compounds in Water Ultraviolet Spectra*, (2009) http://www.imoa.info/download_files/HSE/Uv_analysis_Mo_compounds.pdf.
40. P. L. Brown and C. Ekberg, *Hydrolysis of Metal Ions*, Wiley-VCH Verlag GmbH & Co., Editor, (2016) https://onlinelibrary.wiley.com/doi/book/10.1002/9783527656189.
41. E. Shembel et al., *J. Solid State Electrochem.*, **9**, 96 (2005).
42. D. Sinkeviciute, J. Baltrusaitis, and N. Dukstiene, *J. Solid State Electrochem.*, **15**, 711 (2011).
43. R. L. Miller, B. L. Wesley, and N. E. Peters, *Specific Conductance: Theoretical Considerations and Application to Analytical Quality Control*, (1988) https://pubs.usgs.gov/wsp/2311/report.pdf.